Supporting Information

MXene-Driven Augmentation of Hole-Selective Self-Assembled Monolayer Interfaces for Efficient and Stable p-i-n Perovskite Solar Cells

Kyeong Su Kim[§, §§], Jung Jae Do[§, §§], and Jae Woong Jung[§, §§]*

[§]Integrated Education Institute for Frontier Materials (BK21 Four), Kyung Hee University, 1732 Deogyeong-daero, Giheung-gu, Yongin-si, Gyeonggi-do 446-701, Republic of Korea

[§§]Department of Advanced Materials Engineering for Information & Electronics, Kyung Hee University, 1732 Deogyeong-daero, Giheung-gu, Yongin-si, Gyeonggi-do 446-701, Republic of Korea

* Corresponding author: wodndwjd@khu.ac.kr (Prof. J. W. Jung)

Table S1. TRPL fitting results of CsFAPbI$_3$ films with varied hole-selective interlayers.

Hole-selective interlayer	τ_1 (ns)	τ_2 (ns)	A_1	A_2	τ_{avg}*(ns)
no interlayer	2.22	97.91	5137.78	5497.06	95.92
MeO-2PACz	3.97	46.06	5213.93	4024.53	41.83
MeO-2PACz/MXene 0.01 mg/ml	4.42	24.28	6373.24	3648.16	19.49
MeO-2PACz/MXene 0.02 mg/ml	5.49	26.28	5224.25	3748.35	21.59
MeO-2PACz/MXene 0.03 mg/ml	6.03	49.05	5307.1	3318.05	41.99

Table S2. Photovoltaic parameters of PSCs with different concentrations of MXene onto MeO-2PACz hole-selective interfaces.

Con. MXene [mg ml^{-1}]	V_{OC} [V]	J_{SC} [mA cm^{-2}]	Integrated J_{SC} [mA cm^{-2}]	FF [%]	PCE [%]
-	1.112	23.66	23.09	79.30	20.86
0.005	1.110	23.44	23.11	79.37	20.65
0.008	1.111	23.76	23.06	79.28	20.93

Table S3. Photovoltaic parameters of PSCs with varied concentration of MXene onto MeO-2PACz hole-selective interfaces at different scan directions.
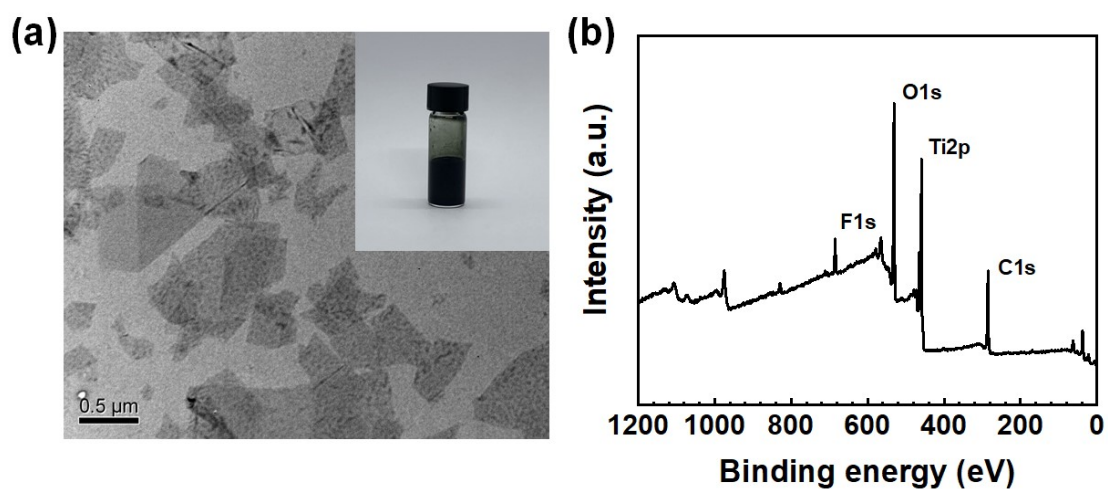
Con. MXene [mg ml^{-1}]	Scan direction	V_{OC} [V]	J_{SC} [mA cm^{-2}]	FF [%]	PCE [%]	HI
0.00	FS	1.09	24.09	0.79	20.74	0.0222
	RS	1.08	24.09	0.78	20.29	
0.01	FS	1.13	24.18	0.82	22.41	0.0087
	RS	1.14	24.18	0.82	22.60	
0.02	FS	1.11	24.26	0.77	20.73	0.0131
	RS	1.11	24.26	0.76	20.46	
0.03	FS	1.10	23.23	0.76	19.42	0.0218
	RS	1.11	23.23	0.77	19.86	

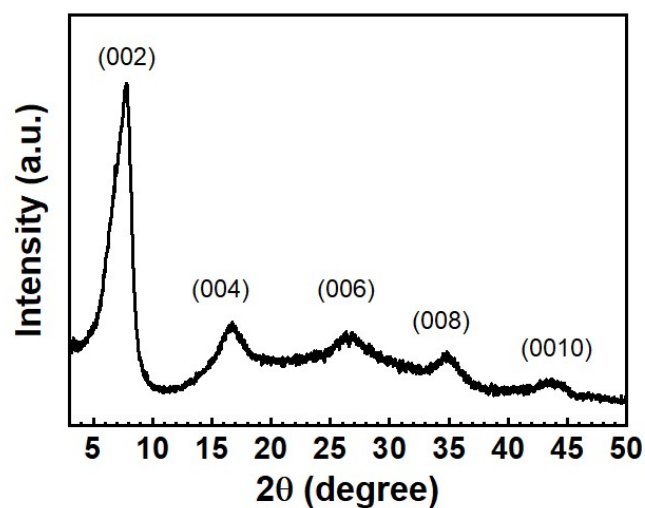**Table S4.** EIS fitting results of PSCs with and without MXene loading in hole-selective interlayers.

Perovskite	EIS fitting		SCLC (hole-only)	
	R_s (Ω)	R_{rec} (Ω)	V_{TFL} (V)	N_t* (10^{15} cm^{-3})
MeO-2PACz	48.1	3827	0.72	3.99
MeO-2PACz/MXene	33.5	5361	0.52	2.22

Table S5. Contact angle result of MeO-2PACz and MXene/MeO-2PACz films on glass substrate.

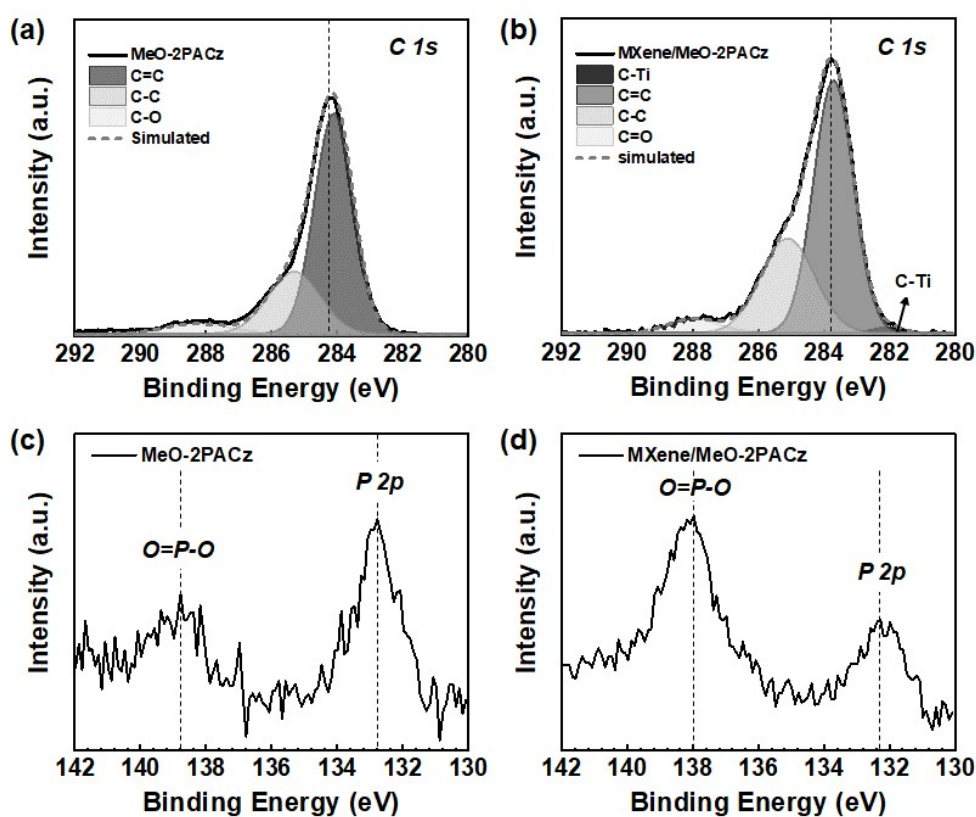| Sample	Contact angle (º)			Surface energy (mJ/m^2)
	DI water	Diiodomethane	Formamide	
MeO-2PACz/glass	41.1 (39.7±2.3)	9.6 (9.0±0.5)	31.3 (31.4±0.8)	56.02
MXene/MeO-2PACz/glass	52.6 (44.8±5.1)	7.8 (10.3±2.3)	34.7 (34.9±0.8)	67.88

Figure S1. (a) TEM image and (b) XPS binding energy spectrum of MXene ($Ti_3C_2T_x$) nanosheets prepared in this work. The photogarphic image of MXene dispersion in water (1 mg/ml) is displayed in inset of Figure S1a.
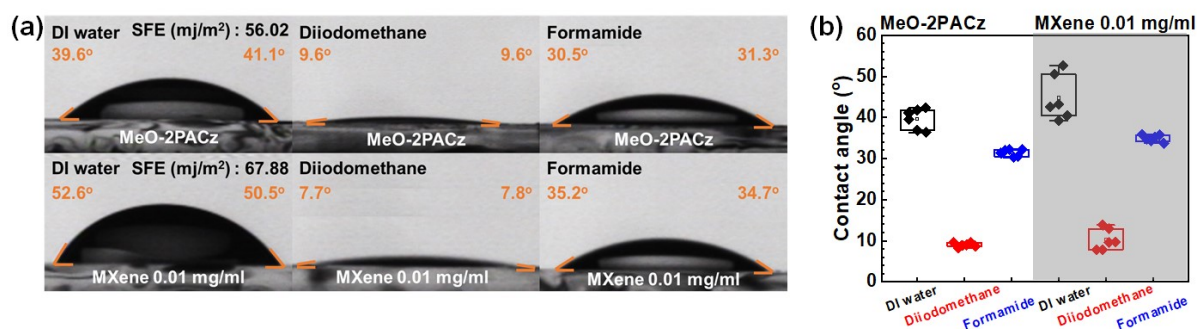

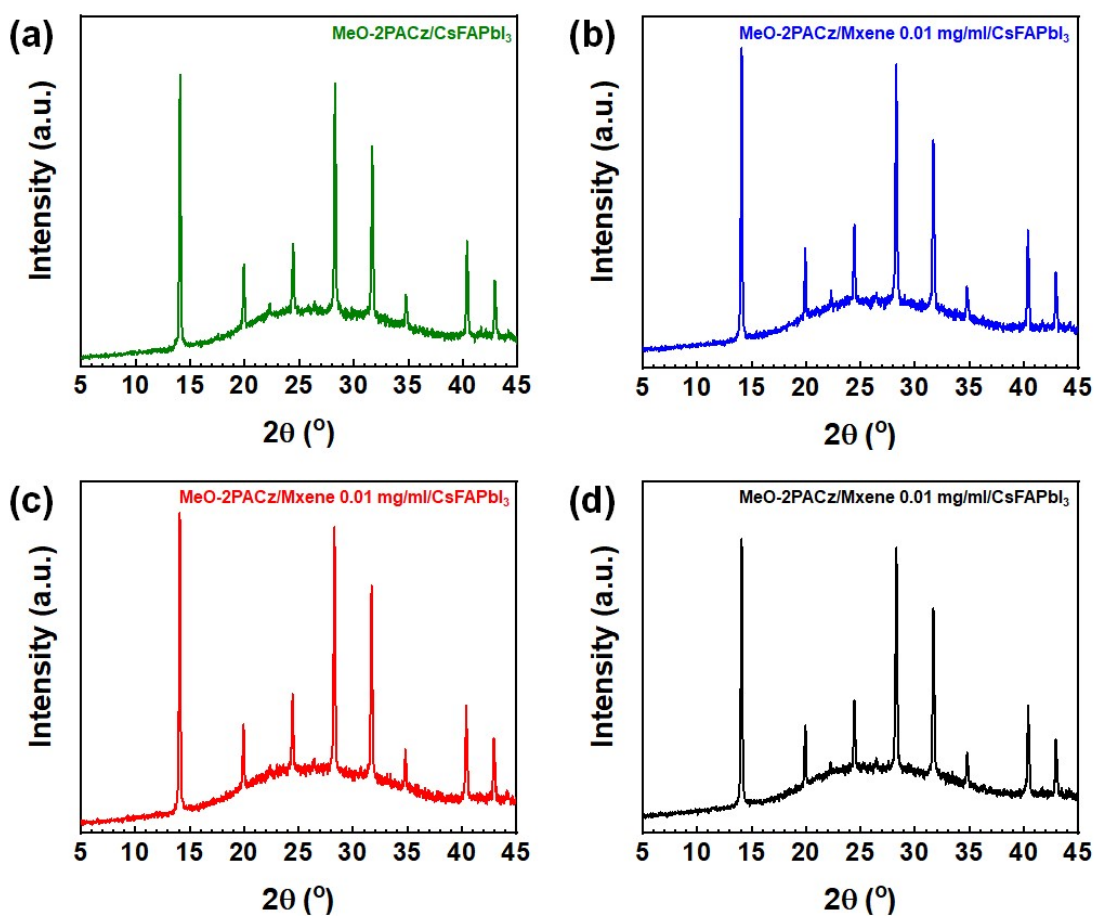**Figure S2.** XRD diffractogram of MXene ($Ti_3C_2T_x$) film prepared in this work.

Figure S3. Photographic images of MXene (bulk), MeO-2PACz, MeO2PACz/MXene films with varied concentration of MXene deposition.

Figure S4. High-resolution XPS binding energy spectra of prstine MeO-2PACz film (a and c) and MXene/MeO-2PACz film (b and d) for C1s (a and b) and P 2p (c and d), respectively.

Figure S5. (a) Photographic images of contact angle of MeO-2PACz and MeO-2PACz/SAM for DI water, diiodomethane, and formamide, and (b) the summary of contact angles from 8 different samples in each condition.

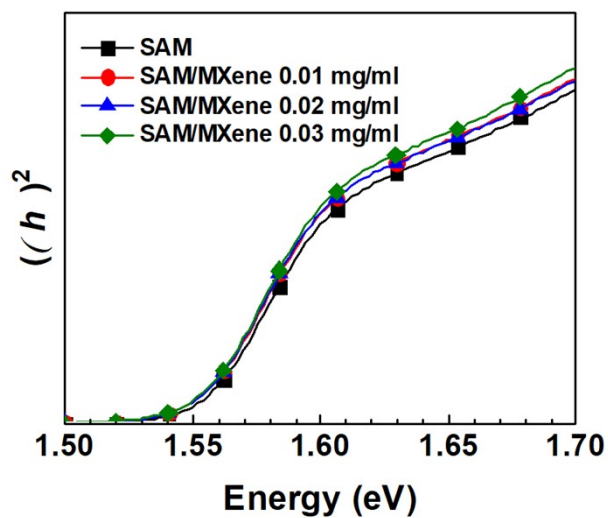**Figure S6.** XRD patterns of CsFAPbI$_3$ perovskite films with varied substrate.

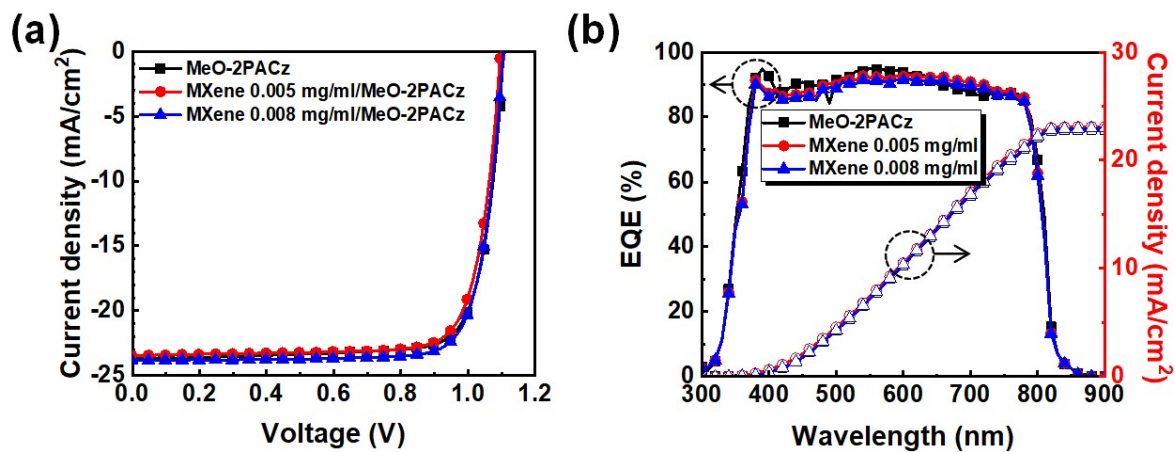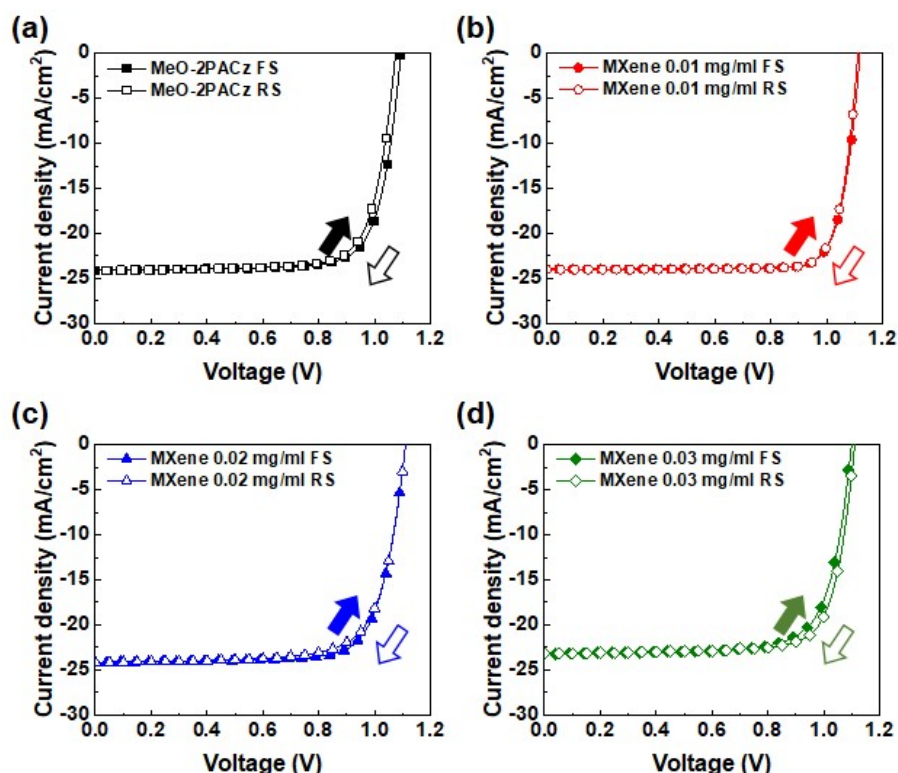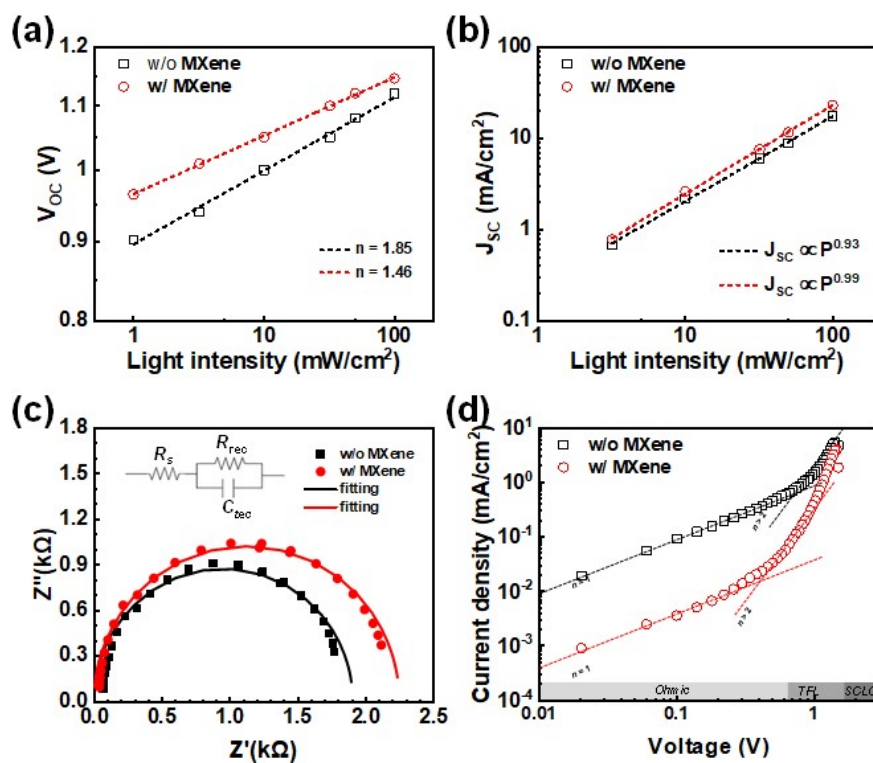**Figure S7.** Tau plots of CsFAPbI$_3$ perovskite films grown on varied substrate.

Figure S8. *J−V* curves (a) and EQE spectra (b) of the devices of PSCs different concentrations of MXene onto MeO-2PACz hole-selective interfaces.

Figure S9. *J–V* curves of devices made of different hole-injecting interfaces with varied scan directions: (a) MeO-2PACz, (b) MXene 0.01 mg/ml on MeO-2PACz, (c) MXene 0.02 mg/ml on MeO-2PACz, (d) MXene 0.03 mg/ml on MeO-2PACz.

Figure S10. (a) Light intensity-dependent V_{OC} decays, (b) J_{SC} decays, (c) Nyquist plots, and (d) SCLC measurements of devices with and without MXene.